

Highly Reduced Polyoxometalates: Ab Initio and DFT Study of $[\text{PMo}_8\text{V}_4\text{O}_{40}(\text{VO})_4]^{5-}$

Xavier López,[†] Coen de Graaf,[‡] Joan Miquel Maestre,[‡] Marc Bénard,[†]
Marie-Madeleine Rohmer,[†] Carles Bo,^{‡,§} and Josep M. Poblet^{*,‡}

Laboratoire de Chimie Quantique, UMR 7551, CNRS and Université Louis Pasteur, 4 rue Blaise Pascal, F-67000 Strasbourg, France, Departament de Química Física i Inorgànica, Universitat Rovira i Virgili, 43005 Tarragona, Spain, and Institut Català d'Investigació Química, Avda, dels Països Catalans s/n, 43007 Tarragona, Spain

Received February 25, 2005

Abstract: DFT and post Hartree–Fock calculations were carried out to characterize the electronic structure of the 10-electron-reduced $[\text{PMo}_8\text{V}_4\text{O}_{40}(\text{VO})_4]^{5-}$ polyoxometalate. This molecule may be viewed as a mixed-metal $\text{PMo}_8\text{V}_4\text{O}_{40}$ Keggin structure capped with four VO units, in which the eight vanadiums form a ring. In mixed V/Mo clusters it is accepted that the first reductions occur at the V^{5+} ions. The BP86 calculations on this modified Keggin anion reveal that the ground state is a septet with the six unpaired electrons delocalized over the eight V centers. The B3LYP calculations and especially the CASSCF technique modify the tendency of the BP86 method, thus reproducing the expected 8/2 distribution. The unpaired electrons residing in the eight vanadiums are antiferromagnetically coupled.

Introduction

The chemistry of medium and large molecular metal oxides, or polyoxometalates (POMs),¹ was mainly restricted for years to the tungsten and molybdenum derivatives, although it has been enriched and broadened in the past decades.² New chemical and structural ingredients are incorporated to this field in order to tune the characteristics of such inorganic systems. Among varied strategies driven nowadays with this goal, one of them is incorporating capping units to a parent structure. This method resides in the addition of M_xO_y groups to the surface of a POM cluster. A handful of capped clusters have been synthesized and characterized in the last 10 years, which are mostly restricted to compounds containing Mo, V, and As atoms. A benchmarking bicapped anion was characterized by Hill and co-workers in the middle 1990s,³ with the formula $[\text{PMo}_{12}\text{O}_{40}(\text{VO})_2]^{5-}$. The special electronic features of this anion were analyzed by means of the DFT methodology by Maestre et al.,⁴ which reproduced and explained the particular electronic nature of such polyanion.

Other derivatives with similar chemical compositions containing capping units have been reported, either constructed upon a single-addenda or a substituted parent POM core.^{5–14} Novel capped clusters containing V and Ge atoms were reported by Whitfield et al. in 2003.¹⁵ $[\text{Ge}_4\text{V}_{16}\text{O}_{42}(\text{OH})_4]^{8-}$ constitutes the first example of Ge_2O_7 capping units incorporated to vanadate derivatives based on the Keggin anion.

In 1999, Xu et al. reported a novel POM containing for the first time *four* capping groups, namely the $[\text{PMo}_8\text{V}_4\text{O}_{40}(\text{VO})_4]^{5-}$ cluster (**1**),¹⁶ shown in Figure 1A. This species is made up of a $[\text{PMo}_8\text{V}_4\text{O}_{40}]^{7-}$ Keggin-like mixed-metal cluster (Figure 1B) where four VO^{3+} units are added to the 12-metal core. The VO^{3+} entities carry a total charge of +12, which transforms the initial $[\text{PMo}_8\text{V}_4\text{O}_{40}]^{7-}$ anion into the $[\text{PMo}_8\text{V}_4\text{O}_{40}(\text{VO})_4]^{5+}$ cation. The resulting compound was indeed characterized as a 10e[−]-reduced molecule, thus with a net charge of −5. More recently, the same group published a related compound with similar electronic structure¹⁰ and, in 2003, Yuan et al. reported three novel V-capped Keggin derivatives with paramagnetic metal complexes attached to the surface of the cluster.¹⁷ Perhaps, the most important common feature of such compounds is that they are found in highly reduced forms.

* Corresponding author e-mail: josepmaria.poblet@urv.net.

[†] UMR 7551, CNRS and Université Louis Pasteur.

[‡] Universitat Rovira i Virgili.

[§] Institut Català d'Investigació Química.

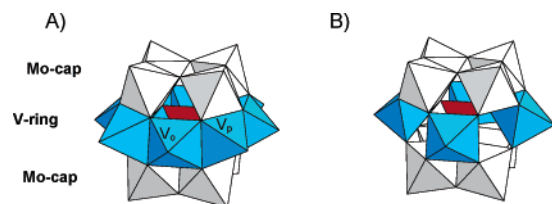


Figure 1. Polyhedral representation of the $[\text{PMo}_8\text{V}_4\text{O}_{40}(\text{VO})_4]^{5-}$ anion (A). Blue polyhedra show the equatorial V_8 -ring of alternating octahedral and pyramidal, V_o/V_p , vanadiums, whereas four molybdenums are located in each polar region. The four V_p are the “capping” units of the parent $[\text{PMo}_8\text{V}_4\text{O}_{40}]$ framework (B) and are formally pentacoordinated in the final cluster. The overall symmetry of the cluster is D_{2d} .

Although the structure reported for **1** is formally a tetracapped Keggin cluster, it may be viewed as an eight-membered equatorial ring of vanadium atoms (V_8 -ring) together with two polar units made of four MoO_6 units each (Figure 1). Such framework contains all-equivalent Mo atoms, whereas two vanadium types may be distinguished: four pseudo-octahedrally coordinated and four in a square-pyramidal environment, which will be labeled as V_o and V_p from now on, respectively. These two types of V centers are alternated within the V_8 -ring. With the analysis of **1** we pursue two objectives: to rationalize reduced mixed-addenda Mo/V derivatives and to progress in the understanding of capped clusters.^{3,4} The present work is based on quantum chemical calculations performed upon the title structure and the subsequent analysis and discussion of the data related to the electronic structure.

Results and Discussion

In general, it is difficult to unequivocally characterize the number and nature of the reduced metal centers in an “electron-rich” polyoxometal cluster.¹⁸ The number of electronic configurations that are energy-accessible by a reduced system is, at least, moderately large within a small energy range. This is commonplace in reduced POMs since the metal electrons reside over a large number of chemically similar metal centers. In particular, difficulties come out in the assignment of oxidation states in mixed oxides of vanadium and molybdenum. Electrochemical reductions and EPR spectroscopy have been frequently used to determine the localization/delocalization of the metal electrons in reduced POMs. For example, Hervé and co-workers found after electrochemical reduction of $\text{XMo}_2\text{VW}_9\text{O}_{40}$ and $\text{XMoV}_2\text{W}_9\text{O}_{40}$ anions ($\text{X} = \text{P}, \text{Si}$) that the V centers are commonly reduced in the first place.¹⁹ In this line of thought, Xu et al., from X-ray diffraction and EPR spectra analysis, claim that the electronic structure for **1** corresponds to the 10 metal electrons delocalized over the whole system. In fact, from valence sum calculations they conclude that all vanadium atoms have an oxidation state of +4. This means that the eight Mo ions share two electrons. The calculations discussed below were performed with the DFT and CASSCF techniques and are aimed at unraveling the electronic structure, e.g., the molecular orbitals sequence and especially the repartition of metal electrons between Mo and V.

DFT Calculations. We carried out a density-functional-theory (DFT) analysis to characterize the electronic structure of **1**. We performed calculations using the exchange-correlation functionals of Becke and Perdew (BP86)²⁰ and the hybrid B3LYP.²¹ The BP86 geometries were optimized, within the constraints of the D_{2d} symmetry, by means of the ADF program²² with a basis set of triple- ζ + polarization quality. The internal or core electrons (O, 1s; P, 1s–2s; V, 1s–2p; Mo, 1s–4d) were frozen and described by single Slater functions. We applied scalar relativistic corrections to them by means of the zeroth-order regular approximation (ZORA) via the core potentials generated with the DIRAC program.²² Open-shell configurations were computed within the unrestricted formalism, and some low-spin open-shell configurations are treated within the Broken Symmetry (BS) approach.²³

The closed-shell configuration, $S = 0$, shows the typical electronic structure common for most POMs, that is, a band of oxo orbitals doubly occupied and a set of metal orbitals well separated in energy. The two lowest metal orbitals, of a_2 and b_1 symmetry, are quasi-degenerate nonbonding combinations of $d_{xy}(\text{Mo})$ orbitals. We found the energy gap between the highest occupied oxo orbital and the first occupied metal orbital to be 1.74 eV (40.1 kcal mol^{−1}), a somewhat smaller value compared to regular Keggin-like molybdates, which feature ~2 eV (~46 kcal mol^{−1}) in most cases at this level of computation.²⁴ At higher energies we find a set of $d_{xy}(\text{V})$ -like orbitals, and the next Mo-like orbital appears more than 1.2 eV (27.7 kcal mol^{−1}) above the first metal orbital (see Figure 2, configuration $S = 0$). The various BP86 calculations performed preferentially give a balanced sharing of the metal electrons, with six for V and four for Mo (6/4), which in principle contradicts the experimental data and also the general assumption that all V^{5+} centers should be reduced before the first Mo center does. The stability of the 6/4 configurations increases, in general, as the number of unpaired electrons grows. Thus, the septet state,²⁵ with the six unpaired electrons delocalized over the eight V atoms, is the most stable 6/4 configuration and was computed to be 19.1 kcal mol^{−1} below $S = 0$. For this septet state, the Mulliken partition scheme assigns spin populations of 0.90e to V_o and 0.78e to V_p . Several BS low-spin open-shell configurations (not represented in Figure 2) were also found to be more stable than $S = 0$, although invariably with a 6/4 configuration. Among these low-spin open-shell calculations, a common feature was observed, namely, the antiferromagnetic coupling of metal electrons delocalized over the V-ring, as shown in Figure 3.

If we promote all the beta spin electrons of the $S = 0$ configuration and accommodate them in higher orbitals to give a $S = 5$ form, the system increases its energy by 28.1 kcal mol^{−1}, thus lying 47.2 kcal mol^{−1} above the septet state ($S = 3$). This high-spin state is still a 6/4 form as illustrated in Figure 2. The lowest 8/2 state calculated, a triplet ($S = 1$) computed +37.7 kcal mol^{−1} above $S = 0$, confirms that the 6/4 configuration is the most stable with the BP86 functional.

Table 2 contains computed interatomic distances for the title cluster. For comparison, the table also includes the corresponding X-ray values reported in ref 16. The reader

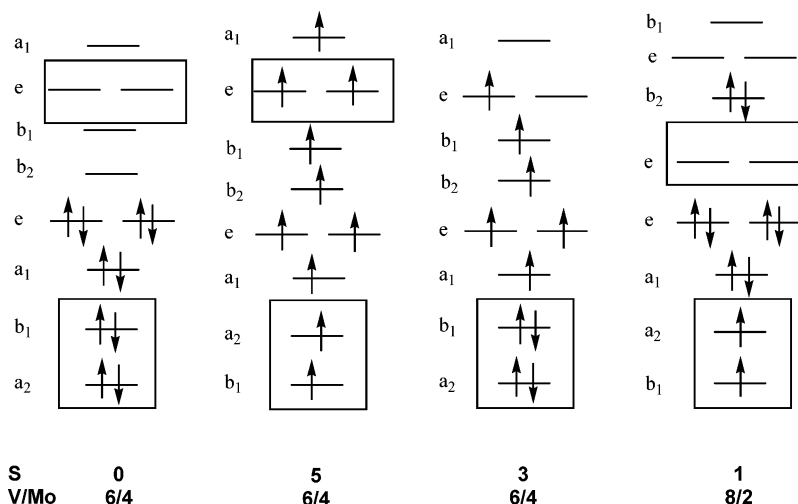


Figure 2. Molecular orbitals representation of the lowest lying metal orbitals of the title compound studied at the BP86 level. The boxes contain orbitals with Mo character. The spin (S) and the V/Mo electron distribution are shown, whereas the relative energies are listed in Table 1. There is no energy scaling in the picture. Only the case $S = 0$ was computed with the restricted DFT formalism.

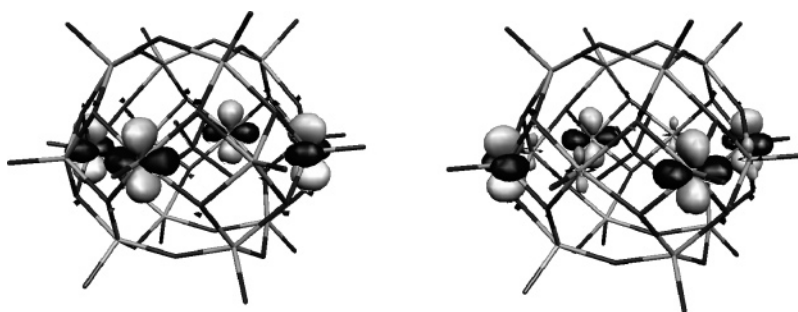


Figure 3. 3D representation of the alpha (left) and beta (right) spatial parts of a symmetry-adapted $d_{xy}(\text{V})$ -like orbital of a_1 symmetry showing the alternate localization in the V_8 -ring computed with the unrestricted DFT formalism.

Table 1. Electronic Parameters for $[\text{PMo}_8\text{V}_4\text{O}_{40}(\text{VO})_4]^{5-}$ Computed at the BP86 Level

configuration V/Mo ^a	6/4	6/4	6/4	8/2
spin (S)	0	5	3	1
relative energy ^b	0.00	+28.1	-19.1	+37.7
spin density ^c				
Mo		0.44	0.018	0.27
V _o		0.95	0.90	0.82
V _p		0.89	0.78	-0.78

^a Number of metal electrons residing on d-V and d-Mo orbitals.
^b kcal mol⁻¹. ^c Spin density per atom.

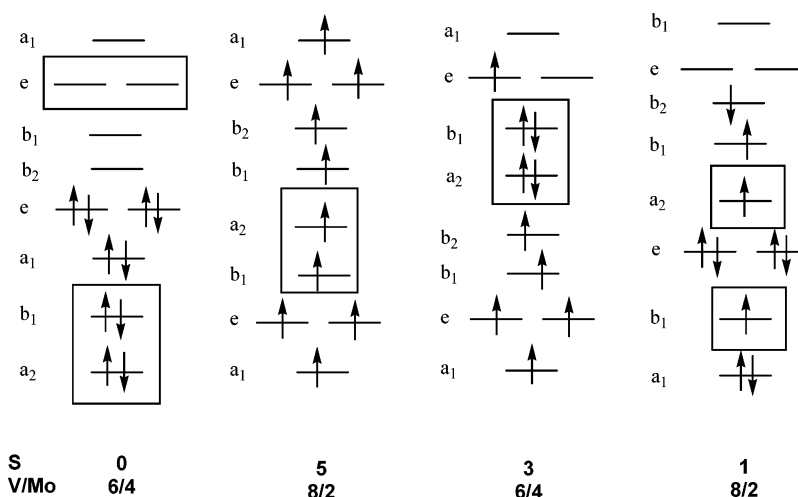
may observe that the geometry does not change significantly upon variations in the electronic configuration and that the computed distances agree fairly well with the experimental ones. For the type of molecules and computation methods discussed here, the largest deviation between experimental and computed values takes place in the terminal M–O bonds. Hence, for example, the computed terminal Mo–O bond is about 0.06 Å longer than the X-ray.

Taking the reference of the electronic configurations studied with the BP86 functional, we also analyzed the title structure at the B3LYP level. We made use of the Gaussian03 package²⁶ to obtain energies for several states employing DZ basis sets together with the Los Alamos effective core potentials for the metal atoms. As in the BP86 calculations, the geometries were fully optimized under the constraints

of the D_{2d} symmetry group. The values in Table 2 clearly show that the two functionals give similar geometries. On the other hand, the results obtained illustrate that the 6/4 electronic distribution, the lowest in energy with BP86, is not the most stable with the hybrid functional. Using B3LYP, the closed-shell calculation with $S = 0$ also locates six and four electrons over vanadiums and molybdenums, respectively, but this configuration is 125 kcal mol⁻¹ less stable than the high-spin 8/2 distribution of the metal electrons ($S = 5$, showed in Figure 4). The $S = 3$ calculation, with formally four paired electrons over Mo atoms and six electrons delocalized over vanadiums, was found 34.5 kcal mol⁻¹ above the $S = 5$ state. Finally, the BS triplet state ($S = 1$) strongly competes with $S = 5$ since it was computed only 0.38 kcal mol⁻¹ above the all-spin-up form. The atomic spin populations computed for vanadiums with the Mulliken method are alternatively $\pm 1.14e$ for V_o and V_p sites. These 8/2 configurations and others with the same electron repartition were computed with the BP86 functional, but they were never found competitive in energy with respect to the 6/4 pattern. Notice from the values in Tables 1 and 3 that the incorporation of the exact exchange functional through a hybrid functional in the calculations favors the localization of the electrons on the vanadium ions. This is an important result since it indicates that the B3LYP functional reproduces the localization of the electrons in mixed V/Mo POMs more

Table 2. Selected Distances (in Å) Computed for the Most Stable States for 6/4 and 8/2 Configurations of the $[\text{PMo}_8\text{V}_4\text{O}_{40}(\text{VO})_4]^{5-}$ Anion

	BP86		B3LYP		X-ray ^b
configuration V/Mo ^a	6/4	8/2	6/4	8/2	
spin (S)	3	1	3	5	
Mo–Mo	3.47–3.74	3.44–3.76	3.48–3.73	3.50–3.76	3.48–3.62
V–V	3.01	3.02	3.02	3.06	2.90–3.03
Mo–V	3.06	3.04	3.09	3.08	3.02
Mo–O(term)	1.73	1.74	1.74	1.73	1.67
V–O(term)	1.62–1.63	1.62–1.63	1.60–1.63	1.61–1.62	1.59–1.66
P–Mo	3.67	3.64	3.67	3.66	3.59–3.64
P–V	3.68–4.11	3.72–4.11	3.62–4.16	3.69–4.20	3.60–4.06

^a Number of metal electrons residing on d-V and d-Mo orbitals. ^b Reference 16.**Figure 4.** The same scheme as in Figure 2 but using the B3LYP functional. Energy data are listed in Table 2.**Table 3.** Electronic Parameters for $[\text{PMo}_8\text{V}_4\text{O}_{40}(\text{VO})_4]^{5-}$ Computed at the B3LYP Level

configuration V/Mo ^a	6/4	6/4	8/2	8/2 ^d
spin (S)	0	3	5	1
relative energy ^b	+125	+34.5	0.00	+0.38
spin density ^c				
Mo		0.01	0.32	0.31
V _o		0.74	1.13	1.14
V _p		1.04	1.16	-1.14

^a Number of metal electrons residing on d-V and d-Mo orbitals.^b kcal mol⁻¹. ^c Spin density per atom. ^d State computed within the broken symmetry approach.

accurately than pure GGA functionals. For an extensive description of the localization/delocalization problem see for example the papers in ref 27. To evaluate the effect of the basis set upon the results, we tried to obtain some of the configurations given in Figures 3 and 4 with the BP86 functional and the DZ GTO-basis set used in the B3LYP calculations. However, we were unable to converge any 8/2 configuration with the former functional. At this level of computation, the energy difference between the high ($S = 5$) and low spin ($S = 0$) states for the 6/4 distribution (Figure 2) was computed to be 20 kcal mol⁻¹, thus ~ 8 kcal mol⁻¹ smaller than the difference found with the TZP STO-basis set.

The most noteworthy result is that the nature of the orbitals involved in the delocalization of the metal electrons is roughly the same with the two functionals used; however, the relative energy of the electronic configurations varies

notably depending on the method applied. Otherwise to the BP86 functional, B3LYP—which includes the exact electron exchange—tends to stabilize the 8/2 configurations with respect to the 6/4 repartition. In addition, the occupied d-orbitals of the Mo atoms appear preferentially at higher energies in comparison to vanadium d-orbitals, except for the closed-shell 6/4 distribution. In this latter configuration, the molecular orbitals sequence and nature are the same, thus indicating that the most remarkable differences between these two functionals appear when open shells are considered and, especially, when the molecular net spin is large.

Ab Initio Post-Hartree–Fock Calculations. To properly represent the distribution of the unpaired metal electrons in $[\text{PMo}_8\text{V}_8\text{O}_{44}]^{5-}$, one may tentatively improve the description by approaching the problem from a different viewpoint. The DFT calculations discussed above indicate that there are many different electronic configurations in a small energy interval. Therefore, it might be more consistent to include all these near-degeneracies in the description of the electronic charge distribution from the start in a well-defined way. Despite the large size of the POM under study, we employ complete active space self-consistent field (CASSCF) calculations as implemented in the MOLCAS 5.4 code.^{28–29} This wave function based method has two important advantages above DFT. In the first place, it gives a rigorous description of the spin states, i.e., the N -electron wave function is an eigenfunction of the S^2 operator. Second, it treats all

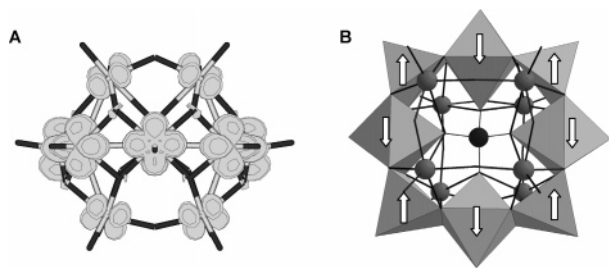


Figure 5. (A) View along the V_8 -equatorial plane of the CASSCF alpha spin density for the singlet ground state of $[PMo_8V_4O_{40}(VO)_4]^{5-}$. (B) Perpendicular view of the V_8 -ring (polyhedra) showing the antiparallel coupling found for the eight vanadium electrons (grey spheres represent molybdenum centers).

important electronic configurations on an equal footing. This means that all so-called nondynamical electron correlation is accounted for. It is, however, very difficult to include the dynamical electron correlation (the description of the discontinuity in the gradient of the wave function when two electrons are close to each other) in the CASSCF wave function due to the size of the molecule. Nevertheless, the CASSCF approach is usually sufficient for an accurate description of the electron distribution of a given N-electron state. The dynamical electron correlation can have a strong effect on the relative energy of different states but does not change the character of these states.^{30–31}

CASSCF calculations were performed on the high-spin coupled ($S = 5$) and the low-spin (singlet) coupled electronic states using the same DZ basis set as in the B3LYP calculations. The active space contains 10 electrons and 12 orbitals. The active orbitals are linear combinations of either V-centered 3d orbitals or combinations of Mo-4d orbitals. In principle, 16 linear combinations can be constructed with these atomic d-orbitals (8 Mo-4d and 8 V-3d). However, the active space has been limited to the 12 molecular orbitals that are lowest in energy, excluding the four out-of-phase linear combinations of Mo-4d orbitals. The optimization of both the CI expansion and the molecular orbital coefficients ensures an unbiased treatment of the different electron distributions over V and Mo. The outcomes of the CASSCF calculations on the high-spin state indicate a 8/2 distribution of the unpaired electrons over the V and Mo centers, respectively. The Mulliken spin populations for the two different V centers are 0.98 e (i.e. there are eight unpaired electrons in the V_8 -ring) and 0.22 for Mo, consistent with two electrons delocalized over the eight Mo centers.

The singlet state is slightly lower (1.2 kcal mol⁻¹) in energy with respect to the undecaplet state, although it is expected that this energy difference increases when dynamical electron correlation is accounted for. The character of the unpaired spin distribution in the singlet state cannot be assessed through the Mulliken spin populations since these are strictly zero for a singlet spin eigenfunction. However, the character of the active orbitals and the natural occupation numbers indicate that this state can be characterized by an antiferromagnetic alignment of 10 unpaired electrons with a 8/2 spin distribution over V and Mo. The alpha spin density depicted in Figure 5 clearly shows how each V has an

equivalent number of unpaired alpha electrons and that the spin density of the Mo is smaller. Finally, we would like to illustrate the intrinsic multiconfigurational character of the singlet state by reminding that the CI expansion has 80 configuration state functions with $|c_i|^2 > 0.05$ and that the largest CI coefficient is only 0.1737, less than 3% of the total wave function.

Conclusions

The complex problem of the highly reduced polyoxometalates containing V and Mo atoms was faced by means of the ab initio and DFT methodologies. We optimized the geometry of the closed-shell electronic configuration of $[PMo_8V_4O_{40}(VO)_4]^{5-}$ with the DFT/BP86 methodology. At this level of calculation, six out of the 10 metal electrons are delocalized over the V-ring and the other four over the Mo centers (6/4 sharing). Since, in general, it is assumed that V^{5+} ions are reduced before the Mo^{6+} centers, we performed B3LYP and ab initio calculations to check the possible outcomes found in the BP86 description of the electron distribution. Both the B3LYP and CASSCF results eventually change the tendency of the DFT/BP86 method, thus reproducing the expected 8/2 configuration. Although most of the theoretical studies reported on polyoxoanions have been carried out using the BP86 functional the present results suggest that mixed vanadium–molybdenum anions are better described through a hybrid functional. Another appealing characteristic arising from all our calculations is the antiferromagnetic coupling that some metal electrons feature. The eight electrons residing in the equatorial V_8 -ring feature a spin-up/spin-down alternate conformation.

Polyoxomolybdates exhibit an extreme variety of complicated structures.³² Through self-assembly mechanisms mixed-valence giant molecules can be formed. The case herein discussed reveals that the study of the electronic structure of mixed-valence vanadomolybdates is not straightforward and suggests that in the modeling of molybdates constituted by hundreds of atoms the size of the anion is not the unique difficulty to overcome.

Acknowledgment. This work was supported by the Spanish MCyT (BQU2002-04110-C02-01) and the CIRIT of the Generalitat of Catalonia (SGR01-00315). Some calculations have been carried out in the Centre Universitaire Régional de Ressources Informatiques (CURRI, Université Louis Pasteur). X.L. also thanks the Spanish MEC for a postdoctoral grant (EX2004-0113).

Supporting Information Available: Coordinates for the $[PMo_8V_4O_{40}(VO)_4]^{5-}$ structure computed at the B3LYP level. This material is available free of charge via the Internet at <http://pubs.acs.org>.

References

- (1) Pope, M. T. *Heteropoly and Isopoly Oxometalates*; Springer-Verlag: Berlin, 1983.
- (2) Borrás-Almenar, J. J.; Coronado, E.; Müller, A.; Pope, M. T. *Polyoxometalate Molecular Science*; Kluwer Academic Publishers: Dordrecht, The Netherlands, 2003.

- (3) Chen, Q.; Hill, C. L. *Inorg. Chem.* **1996**, 35, 2403.
- (4) Maestre, J. M.; Poblet, J. M.; Bo, C.; Casañ-Pastor, N.; Gómez-Romero, P. *Inorg. Chem.* **1998**, 37, 3444.
- (5) Khan, M. I.; Zubieta, J. *Inorg. Chim. Acta* **1992**, 193, 17.
- (6) Xu, Y.; Xu, J. Q.; Yang, G. Y.; Wang, T. G. Xing, Y.; Lin, Y. H.; Jia, H. Q. *Polyhedron* **1998**, 17, 2441.
- (7) Dolbecq, A.; Cadot, E.; Eisner, D.; Sécheresse, F. *Inorg. Chem.* **1999**, 38, 4217.
- (8) Luan, G. Y.; Li, Y. G.; Wang, E. B.; Han, Z. B. *Inorg. Chem. Commun.* **2001**, 4, 632.
- (9) Müller, A. Z. *Anorg. Allg. Chem.* **1994**, 620, 599.
- (10) Xu, Y.; Zhu, D.-R.; Guo, Z.-J.; Shi, Y.-J.; Zhang, K.-L.; You, X.-Z. *J. Chem. Soc., Dalton Trans.* **2001**, 772.
- (11) Huang, G. Q.; Zhang, S. W.; Wei, Y. G.; Shao, M. C. *Polyhedron* **1993**, 12, 1483.
- (12) Khan, M. I.; Chen, Q.; Zubieta, J. *Inorg. Chim. Acta* **1993**, 212, 199.
- (13) Khan, M. I.; Chen, Q.; Zubieta, J. *Inorg. Chem.* **1993**, 32, 2924.
- (14) Müller, A.; Beugholt, C.; Kögerler, P.; Bögge, H.; Bud'ko, S.; Luban, M. *Inorg. Chem.* **2000**, 39, 5176.
- (15) Whitfield, T.; Wang, X.; Jacobson, A. J. *Inorg. Chem.* **2003**, 42, 3728.
- (16) Xu, Y.; Zhu, H.-G.; Cai, H.; You, X.-Z. *Chem. Commun.* **1999**, 787.
- (17) Yuan, M.; Li, Y.; Wang, E.; Tian, C.; Wang, L.; Hu, C.; Hu, N.; Jia, H. *Inorg. Chem.* **2003**, 42, 3670.
- (18) Poblet, J. M.; López, X.; Bo, C. *Chem. Soc. Rev.* **2003**, 32, 297.
- (19) Cadot, E.; Fournier, M.; Tézé, A.; Hervé, G. *Inorg. Chem.* **1996**, 35, 282.
- (20) Becke, A. D. *J. Chem. Phys.* **1986**, 84, 4524; *Phys. Rev. A* **1988**, 38, 3098. Perdew, J. P. *Phys. Rev. B* **1986**, 33, 8822. Perdew, J. P. *Phys. Rev. B* **1986**, 34, 7406.
- (21) Becke, A. D. *J. Chem. Phys.* **1993**, 98, 5648. Lee, C.; Yang, W.; Parr, R. G. *Phys. Rev. B* **1988**, 37, 785.
- (22) ADF 2003.01, Department of Theoretical Chemistry, Vrije Universiteit, Amsterdam. Baerends, E. J.; Ellis, D. E.; Ros, P. *Chem. Phys.* **1973**, 2, 41. Versluis, L.; Ziegler, T. *J. Chem. Phys.* **1988**, 88, 322. Te Velde, G.; Baerends, E. J. *J. Comput. Phys.* **1992**, 99, 84. Fonseca Guerra, C.; Snijders, J. G.; Te Velde, G.; Baerends, E. J. *Theor. Chem. Acc.* **1998**, 99, 391.
- (23) Noodleman, L. *J. Chem. Phys.* **1981**, 74, 5737. Noodleman, L.; Davidson, E. R. *Chem. Phys.* **1986**, 109, 131. Noodleman, L.; Case, D. A. *Adv. Inorg. Chem.* **1992**, 38, 423. Noodleman, L.; Pen, C. Y.; Case, D. A. Mouesca, J. M. *Coord. Chem. Rev.* **1995**, 144, 199.
- (24) López, X.; Maestre, J. M.; Bo, C.; Poblet, J. M. *J. Am. Chem. Soc.* **2001**, 123, 9571.
- (25) This electronic state could stabilize through a first-order Jahn–Teller effect; however, our experience on similar cases points out that the stabilization upon distortion would be small (Maestre, J. M.; López, X.; Bo, C.; Casañ-Pastor, N.; Poblet, J. M. *J. Am. Chem. Soc.* **2001**, 123, 3749).
- (26) *Gaussian 03, Revision C.02*, Frisch, M. J.; Trucks, G. W.; Schlegel, H. B.; Scuseria, G. E.; Robb, M. A.; Cheeseman, J. R.; Montgomery, J. A., Jr.; Vreven, T.; Kudin, K. N.; Burant, J. C.; Millam, J. M.; Iyengar, S. S.; Tomasi, J.; Barone, V.; Mennucci, B.; Cossi, M.; Scalmani, G.; Rega, N.; Petersson, G. A.; Nakatsuji, H.; Hada, M.; Ehara, M.; Toyota, K.; Fukuda, R.; Hasegawa, J.; Ishida, M.; Nakajima, T.; Honda, Y.; Kitao, O.; Nakai, H.; Klene, M.; Li, X.; Knox, J. E.; Hratchian, H. P.; Cross, J. B.; Bakken, V.; Adamo, C.; Jaramillo, J.; Gomperts, R.; Stratmann, R. E.; Yazyev, O.; Austin, A. J.; Cammi, R.; Pomelli, C.; Ochterski, J. W.; Ayala, P. Y.; Morokuma, K.; Voth, G. A.; Salvador, P.; Dannenberg, J. J.; Zakrzewski, V. G.; Dapprich, S.; Daniels, A. D.; Strain, M. C.; Farkas, O.; Malick, D. K.; Rabuck, A. D.; Raghavachari, K.; Foresman, J. B.; Ortiz, J. V.; Cui, Q.; Baboul, A. G.; Clifford, S.; Cioslowski, J.; Stefanov, B. B.; Liu, G.; Liashenko, A.; Piskorz, P.; Komaromi, I.; Martin, R. L.; Fox, D. J.; Keith, T.; Al-Laham, M. A.; Peng, C. Y.; Nanayakkara, A.; Challacombe, M.; Gill, P. M. W.; Johnson, B.; Chen, W.; Wong, M. W.; Gonzalez, C.; and Pople, J. A. Gaussian, Inc., Wallingford, CT, 2004.
- (27) Pickett, W. E. *Rev. Mod. Phys.* **1989**, 61, 433. Mattheiss, L. F. *Phys. Rev. B* **1994**, 49, 14050. Cabrero, J.; Calzado, C. J.; Maynau, D.; Caballol, R.; Malrieu, J. P. *J. Phys. Chem. A* **2002**, 106, 8146. Pacchioni, G.; Frigoli, F.; Ricci, D.; Weil, J. A. *Phys. Rev. B* **2001**, 63, 054102.
- (28) Roos, B. O.; Taylor, P. R.; Siegbahn, P. E. M. *Chem. Phys.* **1980**, 48, 157.
- (29) Andersson, K.; Barysz, M.; Bernhardsson, A.; Blomberg, M. R. A.; Cooper, D. L.; Fleig, T.; Fülscher, M. P.; de Graaf, C.; Hess, B. A.; Karlström, G.; Lindh, R.; Malmqvist, P.-Å.; Neogrády, P.; Olsen, J.; Roos, B. O.; Schimmelpfennig, B.; Schütz, M.; Seijo, L.; Serrano-Andrés, L.; Siegbahn, P. E. M.; Ståhring, J.; Thorsteinsson, T.; Veryazov, V.; Widmark, P.-O. MOLCAS version 5.4, Department of Theoretical Chemistry, University of Lund, 2002.
- (30) Roos, B. O.; Ryde, U. In *Comprehensive Coordination Chemistry 2*; Lever, B., Ed.; Elsevier: Amsterdam, The Netherlands, 2003; Vol. 1.
- (31) de Graaf, C.; Sousa, C.; Broer, R. *Phys. Rev. B* **2004**, 70, 235104.
- (32) Müller, A.; Peters, F.; Pope, M. T.; Gatteschi, D. *Chem. Rev.* **1998**, 239.

CT050040Z